INFLUENCE OF THE BOUNDARY CONDITIONS ON THE DIRECT NUMERICAL SIMULATION OF A PLANE TURBULENT JET

Markus Klein, Amsini Sadiki, Johannes Janicka
Department of Mechanical Engineering
Institute for Energy- and Powerplant Technology
Technical University of Darmstadt
D-64287 Darmstadt, Germany
ekt@hrzpub.tu-darmstadt.de

ABSTRACT

A plane turbulent jet at Re=4000 is investigated using Direct Numerical Simulation. The influence of the inflow conditions is pointed out by using an inflow generator (Lee et al., 1992, Lund et al., 1998) which reproduces the turbulence spectra as well as first and second order statistics from a given experiment. The effects of different mean velocity profiles, fluctuation levels and turbulence spectra on the jet development are investigated. A strong dependence of the length of the potential core and the jet spreading rate on the artificial inflow velocity profile has been found.

INTRODUCTION

Turbulent jets have been the subject of experimental and numerical work for over fourty years, because they are used for the evaluation of physical models. For the axisymmetric jet the very extensive measurements of Wygnanski and Fiedler (1975) have been the standard round jet data for a long time. Baker (1980) has discovered by using numerical methods, that the far field data of Wygnanski & Fiedler have not satisfied the constraint of the integrated axial momentum equation. Later, Capp (1983) has found that this discrepancy has been due to the semi-confined enclosure. Nearly two decades later, almost concurrent detailed measurements with more suitable measurements techniques have been carried out by Hussein et al. (1994) and Panchapakesan and Lumley (1993). In contrast to the round jet, according to Bonnet et al. (1998), detailed results newer than those from Gutmark and Wygnanski (1976) are not available for the plane jet, but in view of the above mentioned findings for the axisymmetric jet, the data of Gutmark and Wygnanski (1976) must be also cast in doubt (Bonnet et al., 1998). Furthermore, there is little work about free jets at moderate Reynolds numbers. The fast improvements in computer hardware made the Direct Numerical Simulation of free jets, at least for low Reynolds numbers feasible. Therefore in Klein et al. (2000a)we performed a simulation of a free plane jet at Reynolds numbers varied in the range from 1000-6000 and obtained good agreement with experimental data (Namer and Ötügen, 1988, Gutmark and Wygnanski, 1976). Our simulations supported the observation that the longitudinal fluctuations obtained by Gutmark and Wygnanski (1976) are about 20 % too high. Altough we obtained good agreement with experimental data comparing self similarity profiles, the prediction of the length of the potential core and the jet spreading rate were still unsatisfactory. The most probable explanation for this discrepancy seemed to be the use of non realistic inflow conditions, whose choice is still an unsolved problem for spatially developing simulations (Lund et al., 1998). Against this background we varied systematically the inflow conditions by using an inflow generator (Lee et al., 1992, Lund et al., 1998), which reproduces a given turbulence spectra as well as first and second order statistics, or alternatively we extracted data from a separate channel flow DNS. Particularly regarding the near field of the jet, this work constitutes also a basis for an investigation of primary breakup of liquid jets in the framework of two-phase flows (See Klein et al., 2000b, Klein et al., 2001).

NUMERICAL TECHNIQUE

The Navier-Stokes equations for a Newto-

nian incompressible fluid are solved, using a finite volume technique on a cartesian mesh. The variables are located on a staggered grid. For spatial discretisation central differences are used. Temporal discretisation is a third order Runge-Kutta-scheme. The Poisson equation is inverted using a direct 'fast-elliptic-solver'.

The turbulent plane jet is simulated with a Reynolds number $Re = U_0\ D/\nu$ of 4000, where U_0 denotes the bulk velocity at the inlet, D the nozzle width and ν the kinematic viscosity. The extension of the computational domain in axial (x), homogenous (y) and vertical (z) direction is $20D \times 8D \times 20D$. The computational domain is resolved with $257 \times 64 \times 512 \approx 8.4 \cdot 10^6$ grid points, where the nozzle is resolved with 50 cells and the grid is stretched at the lateral boundaries. At the outflow Neumann boundary conditions for the velocity and the pressure are prescribed. Setting the pressure to zero at the top and the bottom boundaries and interpolating the tangential velocities constantly allows for mass entrainment. Periodic boundary conditions are applied in the homogenous direction. At the inflow boundary the velocity is set to zero outside the nozzle. Inside the nozzle the velocity profile has been choosen from several possibilities described in the next section.

INFLOW BOUNDARY CONDITIONS

For the mean velocity profile we used a

- *top hat profile,*

$$\bar{U} = U_0, \quad \bar{V} = \bar{W} = 0, \tag{1}$$

- *a top hat profile with smoothed edges,*

$$\bar{U} = \frac{U_0}{2} + \frac{U_0}{2} \tanh\left(\frac{z}{2\theta}\right), \tag{2}$$
$$\bar{V} = \bar{W} = 0,$$

  where θ is the momentum thickness and was set to $D/20$ (Ribault et al., 1999),

- *and a developed channel flow profile,* taken from a separate channel flow DNS comparable to that of Kim et al. (1987).

The mean velocity profiles were superimposed with velocity fluctuations taken

- as zero (laminar inflow conditions),
- from a separate channel flow DNS,
- and from the inflow generator.

Laminar inflow conditions means here and in the following that zero fluctuations have been used and has not to be confused with a parabolic velocity profile. For the generation of the inflow data we followed the procedure of Lee et al. (1992) to obtain velocity fluctuations $\mathcal{U}_i$ which approximate a given target spectrum. A three–dimensional energy spectrum, representative for isotropic turbulence, given by

$$E(k) \sim k^4 \exp\left(-2(k/k_0)^2\right) \tag{3}$$

has been used. The energy peak wave number k_0 has been varied in the range from $1, \ldots, 16$. These fluctuations are conditioned such that each distribution has zero mean, unit variance and zero covariance with the other two distributions. Then the velocity field is constructed according to $U_i = \bar{U}_i + a_{ij}\mathcal{U}_j$ where the coefficients a_{ij} are related to the Reynolds stress tensor which should be matched by the inflow data (Lund et al., 1998).

RESULTS AND DISCUSSION

In this section the influence of different inflow parameters on the jet development is discussed.

1. Random Fluctuation Approach

Because the present work follows our earlier investigation in Klein et al. (2000a), let us first recall the previous main results in the following. The configuration was identical to the one already presented above. At the inflow the mean velocity profile from a fully developped channel flow with superimposed random fluctuations has been used. The Reynolds number has been varied in the range from $1000, \ldots, 6000$. The results, which are always nondimensionalised with the local centerline velocity U_{cl} and the jet half width $z_{1/2}$, can be summarized as follows:

- The mean velocity has a gaussian profile independent of Re. We found $C \approx 0.675$

$$\frac{U(z)}{U_{cl}} = \exp(-C \cdot (z/z_{1/2})^2) \tag{4}$$

- The simulations support the observation that the longitudinal fluctuations obtained by Gutmark and Wygnanski (1976) are about 20 % too high.
- The velocity fluctuations as well as the shear stress agreed well with the results obtained by Namer and Ötügen (1988) and

Gutmark and Wygnanski (1976), except for the longitudinal fluctuations in the latter case.

- Generally it is assumed that in the self similar region of the jet the centerline velocity decays like

$$\left(\frac{U_0}{U_{cl}}\right)^2 = C_u \left(\frac{x}{D} - C_{u,0}\right) \qquad (5)$$

and the jet spreads linearly with x, i.e.

$$\frac{z_{1/2}}{D} = C_z \left(\frac{x}{D} - C_{z,0}\right) . \qquad (6)$$

Here C_u denotes the velocity decay constant and C_z the spreading rate. $C_{u,0}$ and $C_{z,0}$ denote the virtual origin of the jet. In contrast to the experimental data of Namer and Ötügen (1988) the virtual origin obtained from (5) and (6) decreases systematically with increasing Re (see Fig. 1). The same is true for the velocity decay constant and the spreading angle (see Fig. 2). Furthermore $C_{u,0}$ and $C_{z,0}$ coincided. Although there is a large scatter in experimental data it seems that the jet spreading rate is underpredicted by approximately 20 %.
- The results show that up to a Reynolds number of 6000 the flow is not independent of Re but close to a converged state.

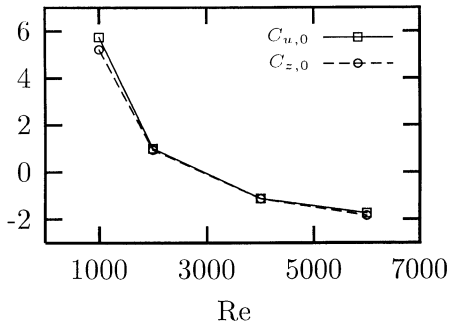

Fig. 1 Virtual origin of jet

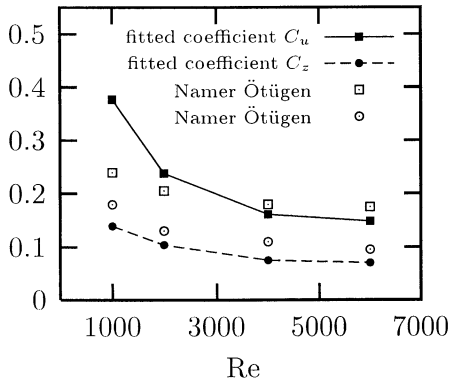

Fig. 2 Decay constant C_u, spreading rate C_z

2. Fluctuations Extracted from a Channel Flow DNS

Although most of the physical behaviour of the plane jet, when varying the Reynolds number, could be predicted in Klein et al. (2000a), it seems that the jet spreading rate was underpredicted by approximately 20 %. The most possible explanation seemed to be unphysical inflow velocity data. Therefore we performed a separate channel flow DNS comparable to that of Kim et al. (1987) in order to extract instationary velocity profiles for the jet simulation. This option was the reason for initially choosing the fully developed channel velocity profile. Although this did not lead to the desired effect, we made a remarkable observation. Fig. 3 shows a comparison of the axial evolution of the longitudinal velocity fluctuations U_{rms}. We compare three plane jet simulations with channel velocity profile at the inlet and with superimposed

- zero fluctuations denoted as CH-laminar,
- random fluctuations scaled to match the channel rms–profiles, (CH-random)
- fluctuations extracted from the channel DNS.

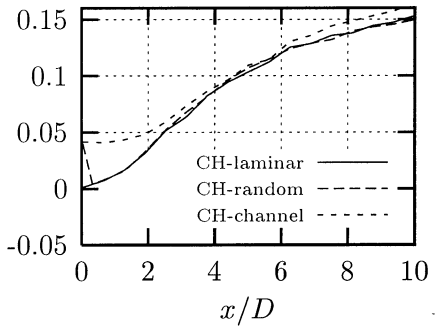

Fig. 3 Axial evolution of U_{rms}

As can be seen from Fig. 3 the fluctuations in the case CH-random drop immediately to a value of approximately zero, where it has to be mentioned that the resolution of this plot is only every fourth data point from the DNS, due to a reduction of data storage. Therefore it is possible that the fluctuation level in this run decreases even faster. This can be explained from a lack of energy in the large scales when using random data fluctuations, where the energy is equally distributed over the whole frequency range. Thus the turbulent kinetic energy is already damped after a half nozzle diameter. Afterwards the profile follows identically the simulation with laminar inflow conditions (CH-laminar). This explains

furthermore a certain independence of the fluctuation level on the simulation results, when using 'white noise' fluctuations. In consideration of this fact the choice of laminar inflow conditions seems to be superior to the random fluctuation approach. Additionally if an iterative solver is used, the number of iterations can be reduced dramatically, see for example Mengler et al. (2001). The use of real turbulence at the inflow (CH-channel) shows a complete different behaviour. In this case the fluctuation level is maintained and increases at the end of the potential core where the shear layer has penetrated into the jet up to the centerline. Unfortunately the spreading rate remained nearly unchanged compared to the simulations CH-random and CH-laminar.

Many experimental studies use a contraction nozzle and therefore report a top-hat profile for the mean velocity. In combination with the inflow generator this yields a more realistic inflow boundary condition, as it will be seen in the next section.

3. Smoothed Top Hat Profile with Fluctuations from the Inflow Generator

Following the ideas of Lee et al. (1992) and Lund et al. (1998), we developped an inflow generator to produce fluctuations representative for isotropic turbulence with a fluctuation level of 2%. These fluctuations where superimposed to a smoothed top hat profile (2) as in Ribault et al. (1999).

3.1 Near field results. Due to our observation, that the distribution of the kinetic energy from the inflow data onto different length scales has an important impact on the evolution of the jet at least in the near field, we studied this influence systematically. Taking the model spectrum (3) the energy peak wave number k_0 has been varied in the range from $1, \ldots, 16$.

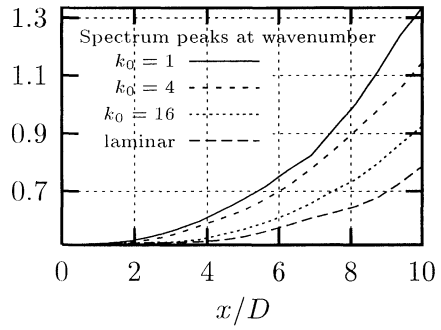

Fig. 4 Streamwise evolution of jet half-width

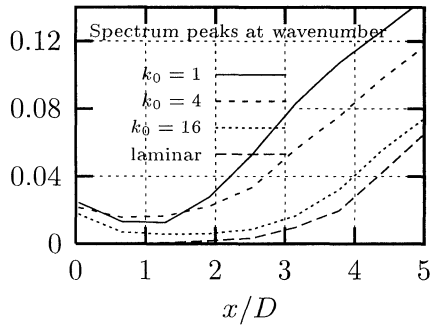

Fig. 5 Axial evolution of U_{rms}

Fig. 4 shows the evolution of the jet half-width in the range $0 \leq x/D \leq 10$ for different energy spectra imposed at the inflow . As expected the jet spreading rate increases, the more kinetic energy is put into the large scales. Comparing the axial evolution of the longitudinal fluctuations in Fig. 5 with the run CH-random in Fig. 3 it is obvious that the data from the inflow generator is much closer to real turbulence, than random fluctuations.

For the cases $k0 = 1$ and the laminar inflow, the jet does not reach a self-similar state until $x/D = 20$. Evaluating a temporal energy spectra of the velocity in the shear layer in the simulation CH-channel and comparing with the actual simulations, the energy distribution seemed to be best represented by the case $k_0 = 4$. Therefore in the following we investigate only this case. Because the initial fluctuation level after the nozzle is not uniform in the experimental literature we made a further simulation with $U_{rms}/U_0 = 0.04$. Evaluating the jet spreading rate C_z and the velocity decay constant C_u as well as the virtual origin in (5), and (6), we found the results summarized in Table 1.

U_{rms}/U_0	C_u	C_z	$C_{u,0}$	$C_{z,0}$
0.02	0.25	0.106	-0.14	-0.77
0.04	0.22	0.098	-2.16	-2.03

Table 1: Velocity decay and jet spreading rate

They are consistent with most of the experimental plane jet literature, where a value of C_z ranging from 0.95 to 1.1 has been found. For the velocity decay constant the scatter is even wider, ranging from $C_u = 0.165$ to $C_u = 0.22$. From Table 1 it can be seen that the fluctuation level at the exit plane effects strongly the jet mixing, which is a well known effect as mentioned in Namer and Ötügen (1988). In our simulations the jet breaks up earlier when the higher fluctuation level is imposed at the jet

exit. The similarity profiles in the far field are nearly identical. We present them for the case $U_{rms}/U_0 = 0.04$ in the next section.

3.2 Far Field Results. In this section we present the far field results for the turbulent jet. The data has been averaged over approximately 12 flow through times. Because the outflow boundary conditions have an upstream influence on the jet, all quantities are evaluated only for $x/D \leq 15$. The presented results are normalized with the local centerline velocity U_{cl} and the jet half-width $z_{1/2}$. They are compared with the experimental findings of Gutmark and Wygnanski (1976) and Namer and Ötügen (1988), denoted in the following GW and NÖ respectively. According to Bonnet et al. (1998), detailed results newer than those from GW are not available for the plane jet. But in view of the findings mentioned in the introduction they must be cast in doubt at least for the longitudinal fluctuations. Unfortunately in the newer data set of NÖ the fluctuaions V_{rms}, W_{rms} as well as the shear stress are not included. Together with the fact that the experiments from NÖ are among others also performed for $Re = 4000$, compared to $Re = 30000$ in GW, this explains the comparison of our simulation results to different data sets.

Fig. 6 shows the axial mean velocity and is very well represented by a gaussian profile (4), as mentioned earlier, and by the data of NÖ. Compared to GW a notable discrepancy is found for $z/z_{1/2} \geq 1.5$. For the corresponding veloctity fluctuations shown in Fig. 7, the situation is different. The DNS supports the observation mentioned in Bonnet et al. (1998) that the results from GW were about 20% too high, whereas a good agreement with NÖ was found. Fig. 8 and Fig. 9 show the other two velocity fluctuations and Fig. 10 the shear stress. Good agreement is also obtained. Fig. 11 shows a one dimensional energy spectra. The inertial subrange and the dissipation range can clearly be seen and there is no pile up of energy at high wave numbers.

Conclusion

A Direct Numerical Simulation of a turbulent plane jet has been presented. Assessment has been made about the effects of different boundary conditions. Comparisons with measurements have yielded good agreement. Especially improvements in the prediction of the jet spreading rate by using more realistic boundary conditions at the inflow, as described above, have been made. This result demonstrates again the importance of realistic boundary conditions. With regard to two phase flows, the work on a Volume-of-Fluid code, enabling the simulation of fluid/fluid interfaces is left for future presentation.

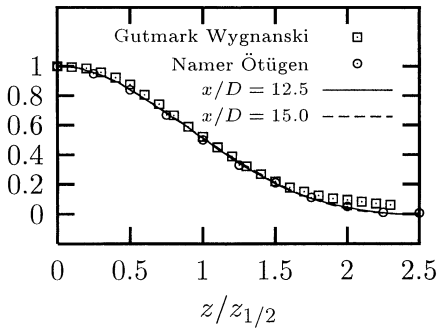

Fig. 6 Mean velocity U_{cl}

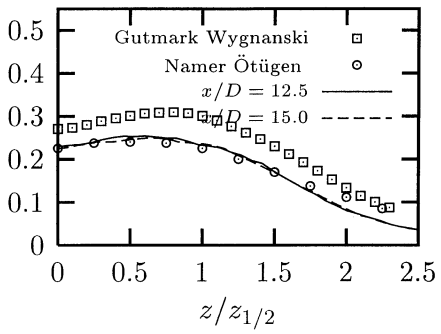

Fig. 7 Mean velocity fluctuations U_{rms}/U_{cl}

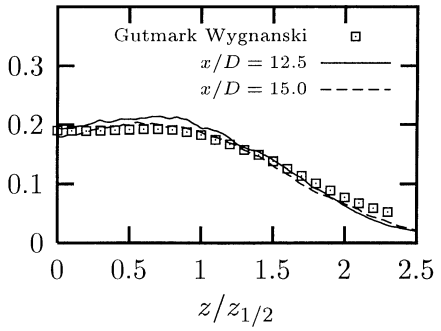

Fig. 8 Mean velocity fluctuations V_{rms}/U_{cl}

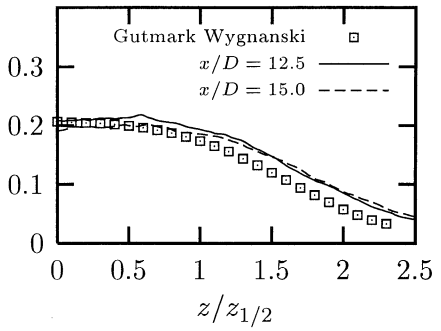

Fig. 9 Mean velocity fluctuations W_{rms}/U_{cl}

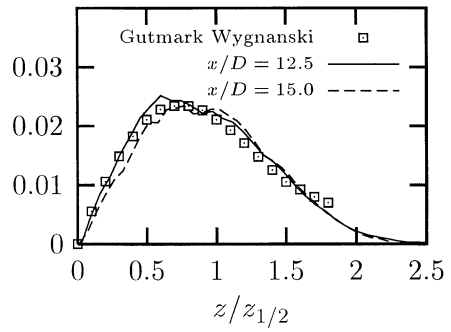

Fig. 10 Shear stress $\overline{u'w'}/U_{cl}^2$

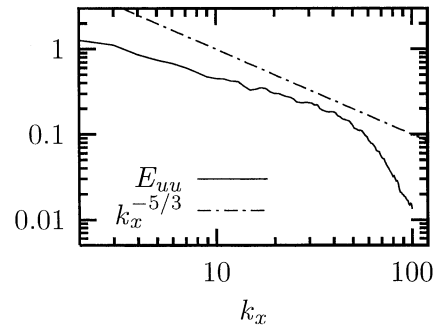

Fig. 11 One dimensional energy spectra

Acknowledgments

The support by the DFG under contract no. JA 544/16 (Schwerpunktprogramm: Fluidzerstäubung und Sprühvorgänge) is gratefully acknowlegded.

References

Baker, C. (1980). *An analysis of the turbulent buoyant jet.* PhD thesis, Pennsylvania State University.

Bonnet, J., Moser, R., and Rodi, W. (1998). *AGARD advisory report 345, A Selection of Test Cases for the Validation of Large Eddy Simulations of Turbulent Flows*, chapter 6.3 Jets. 7 Rue Ancelle, 99200 Neuilly-sur Seine, France.

Capp, S. (1983). *Experimental investigation of the turbulent axisymmetric jet.* PhD thesis, University of Buffalo.

Gutmark, E. and Wygnanski, I. (1976). The planar turbulent jet. *J. Fluid. Mech.*, 73:465–495.

Hussein, H., Capp, S., and George, W. (1994). Velocity measurements in a high-reynolds-number, momentum-conserving axisymmetric , turbulent jet. *Journal of Fluid Mechanics*, 258:31–75.

Kim, J., Moin, P., and Moser, R. (1987). Turbulence statistics in fully developed channel flow at low reynolds number. *J. Fluid Mech.*, 177:133–166.

Klein, M., Sadiki, A., and Janicka, J. (2000a). Direct numerical simulations of plane turbulent jets at moderate reynolds numbers. In *20th IUTAM Congress, ICTAM 2000*, Chicago.

Klein, M., Sadiki, A., and Janicka, J. (2000b). Study of primary jet breakup using direct numerical simulation. In *ILASS-Europe 2000, 16. Annual Conference on Liquid Atomization and Spray Systems*, Darmstadt.

Klein, M., Sadiki, A., and Janicka, J. (2001). Influence of the inflow conditions on the direct numerical simulation of primary breakup of liquid jets. In *ILASS-Europe 2001, 17. Annual Conference on Liquid Atomization and Spray Systems*, Zurich.

Lee, S., Lele, S., and Moin, P. (1992). Simulation of spatially evolving compressible turbulence and the application of taylors hypothesis. *Physics of Fluids*, A4:1521–1530.

Lund, T., Wu, X., and Squires, D. (1998). Generation of turbulent inflow data for spatially-developing boundary layer simulations. *Journal of Computational Physics*, 140:233–258.

Mengler, C., Heinrich, C., Sadiki, A., and Janicka, J. (2001). Numerical prediction of momentum and scalar fields in a jet in cross flow: Comparison of les and second order turbulence closure calculations. In *TSFP2*, Stockholm.

Namer, I. and Ötügen, M. (1988). Velocity measurements in a plane turbulent air jet at moderate Reynolds numbers. *Experiments in Fluids*, 6:387–399.

Panchapakesan, N. and Lumley, J. (1993). Turbulence measurements in axisymmetric jets of air and helium. part 1. air jet. *Journal of Fluid Mechanics*, 246:197–223.

Ribault, C. L., Sarkar, S., and Stanley, S. (1999). Large eddy simulation of a plane jet. *Physics of Fluids*, 11:3069–3083.

Wygnanski, I. and Fiedler, H. (1975). Some measurements in the self-preserving jet. *Journal of Fluid Mechanics*, 38:577–612.